Electromagnetic modeling of waveguide amplifier based on Nd 3+ Si-rich SiO 2 layers by means of the ADE-FDTD method

Christian Dufour, Julien Cardin, Olivier Debieu, Alexandre Fafin, Fabrice Gourbilleau

Nanoscale Research Letters
a SpringerOpen Journal

NANO EXPRESS Open Access

Electromagnetic modeling of waveguide amplifier based on Nd^{3+} Si-rich SiO_2 layers by means of the ADE-FDTD method

Christian Dufour*, Julien Cardin, Olivier Debieu, Alexandre Fafin and Fabrice Gourbilleau

Abstract

By means of ADE-FDTD method, this paper investigates the electromagnetic modelling of a rib-loaded waveguide composed of a Nd^{3+} doped Silicon Rich Silicon Oxide active layer sandwiched between a SiO_2 bottom cladding and a SiO_2 rib. The Auxilliary Differential Equations are the rate equations which govern the levels populations. The Finite Difference Time Domain (FDTD) scheme is used to solve the space and time dependent Maxwell equations which describe the electromagnetic field in a copropagating scheme of both pumping (λ_{pump} = 488 nm) and signal (λ_{signal} = 1064 nm) waves. Such systems are characterized by extremely different specific times such as the period of electromagnetic field ~ 10^{-15} s and the lifetimes of the electronic levels between ~ 10^{-10}s and ~ 10^{-4} s. The time scaling method is used in addition to specific initial conditions in order to decrease the computational time. We show maps of the Poynting vector along the propagation direction as a function of the silicon nanograin (Si-ng) concentrations. A threshold value of 10^{24} Si-ng m^{-3} is extracted below which the pump wave can propagate so that a signal amplication is possible.

Keywords: Silicon nanograin, Silica, Neodymium, ADE-FDTD, Waveguide, amplification

Introduction

The feasibility of optical amplifying waveguide has been for almost two decades the purpose of numerous experimental works [1]. The devices under study were based on an active layer constituted of a silica film co-doped with silicon nanograins (Si-ng) and rare earth ions RE (Er^{3+} in particular) deposited on a substrate and covered by a cladding layer of pure silica. The differences in the optical indices of the three layers ensure the optical guiding. The amplification of a signal is based on an efficient population inversion of the rare earth levels whose energy difference correspond to the signal wavelength. Due to the very low RE signal absorption cross section, a solution has been found using silicon nanoparticles. The physical background lies on two major phenomena: on the one hand, the ability of Si-ng's to absorb efficiently a pumping light and, on the other hand, the effective energy transfer between Si-ng's and RE ions. In this way, a RE population inversion could have been achieved in order to fulfill the amplification function of the device. Despite all these promising features, a net gain is hardly achievable with the former Er^{3+} ions due to their great probability of signal reabsorption from the ground state. This drawback is prevented with the use of Nd^{3+} ions described by a five level scheme since the transition does not involve the ground state. The theoretical studies of the waveguide amplifiers have accounted for both rate population equations and Maxwell equations. In this paper we investigate the ADE-FDTD method applied to a rib-loaded waveguide whose active layer is composed of a silica film co doped with Nd^{3+} ions and silicon nanograins. One of the main issues to be addressed in such systems consists in dealing with extremely different time scales: the populations lifetimes (1 ms) and the electromagnetic field period (10^{-15} s). According to [2,3] we use a time scaling that allows to circumvent this issue. All the lifetimes have been shortened by a factor of 10^6, and consequently the transfer coefficient K has also been divided by the same coefficient. In this paper, we investigate the accuracy of this scaling method through longitudinal and trans-verse maps of the Poynting vector for

* Correspondence: christian.dufour@ensicaen.fr
CIMAP, CEA/CNRS/ENSICAEN/UCBN, 6 Boulevard Maréchal Juin, 14050 Caen Cedex 4, France

several Si-ng concentrations. The applicability of this method is linked to the space and time calculation steps since a reasonable computing time must not be exceeded.

Computational details

We treat the problem within a calculation box as described in Figure 1. Each axis (x,y and z) is divided into space steps (Δx, Δy and Δz respectively).

Four zones appear and will be described hereafter: *i*) the rib-loaded waveguide composed of the active layer (optical index n_{act} = *1.52*) stacked between the SiO_2 cladding and rib (optical index n_{siO_2} = *1.45*), *ii*) the plane containing the electromagnetic field source (z_{source} = 6 Δz), *iii*) the diaphragm (between 7Δz and 10Δz) which transforms the source into a realistic electromagnetic Gaussian field impinging on the waveguide and *iv*) the boundary zone (PML) (4Δz in thickness) characterized by appropriate values of electrical (ρ) and magnetic (σ) conductivities in order to absorb the electromagnetic field so that the box borders do not influence the field in the zone of interest [4].

Lorentz Model for the dielectric susceptibility

Considering a transition between levels i and j we use the Lorentz following relationship which makes the coupling between the polarization density $\mathbf{P}_{i\ j}$, the level populations Ni and N_j in m^{-3} and the total electric field $\mathbf{E}$:

$$\frac{d^2\mathbf{P}_{ij}(t)}{dt^2} + \Delta\omega_{ij}\frac{d\mathbf{P}_{ij}(t)}{dt} + \omega_{ij}^2\mathbf{P}_{ij}(t) = \kappa\,\Delta N_{ij}(t)\mathbf{E}(t) \qquad (1)$$

$\Delta\omega_{ij}$ is the FWHM of the ij transition deduced from photoluminescence measurements according to [5], $\omega_{ij} = \frac{2\pi c}{\lambda_{ij}}$ is the oscillator pulsation linked to the ij transition wavelengh λ_{ij}, $\kappa = \frac{6\pi\varepsilon_0 c^3\gamma_{ij}}{\omega_{ij}^2}$ and γ_{ij} is the ij radiative transition rate in s^{-1} [6,7]. The level populations difference in m^{-3} is given by $\Delta N_{ij} = N_i - N_j$.

In the same way, we describe the polarisation density $\mathbf{P}_{si}$ linked to the silicon level populations N_{Si} (ground level) and N_{Si}^* (excited level),to the oscillator pulsation ω_{Si} and finally to the transition FWHM $\Delta\omega_{Si}$.

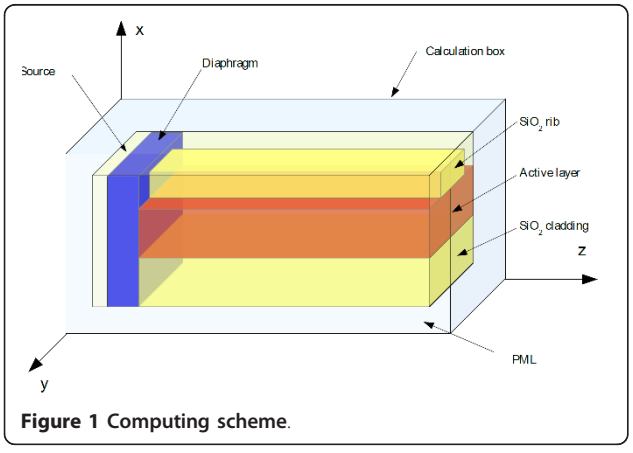

Figure 1 Computing scheme.

Maxwell equations: FDTD numerical method

We start from the Maxwell equation which links the displacement vector $\mathbf{D}$ to the magnetic excitation $\mathbf{H}$:

$$\frac{\partial\mathbf{D}}{\partial t} = \overrightarrow{\text{curl}}\mathbf{H} - \mathbf{J}_e$$

where the current density $\mathbf{J}_e$ is related to $\mathbf{E}$ by $\mathbf{J}_e = \sigma\mathbf{E}$ where σ is the electrical conductivity. Accounting for the relationship between $\mathbf{D}$ and the total polarisation density, $\mathbf{D} = \varepsilon_0\mathbf{E} + \Sigma\,\mathbf{P_{ij}}$ we may write:

$$\frac{\partial\mathbf{E}}{\partial t} = \frac{1}{\varepsilon_0\varepsilon_r}\overrightarrow{\text{curl}}\,\mathbf{H} - \frac{\sigma}{\varepsilon_0\varepsilon_r}\mathbf{E} - \frac{1}{\varepsilon_0\varepsilon_r}\frac{\partial\left(\sum\mathbf{P}_{Si}\right)}{\partial t} \qquad (2)$$

$$\frac{\partial\mathbf{H}}{\partial t} = -\frac{1}{\mu}\overrightarrow{\text{curl}}\mathbf{E} - \frac{\rho}{\mu}\mathbf{H} \qquad (3)$$

All the calculations are performed with real variables. Hence, in order to account for absorption processes other than those due to the level transitions, we characterize (especially for the diaphragm and PML) a specific electric conductivity σ and magnetic conductivity ρ.

Both equations 2 and 3 are solved using the Yee algorithm [8]. The space steps are chosen so that: $\Delta x = \Delta y = \Delta z \ll \lambda_{min}$ (the lowest values among all the wavelengths) Hereafter: $\Delta x = \Delta y = \Delta z$ = 45 nm. The time step Δt must fulfill the condition: $\Delta t \ll \frac{\Delta z}{c}$. Finally the fields inputs (pump and signal) are known as the 'source issue'. Since no perfect source is available, we choose an xy plane at $z_{source} = 6\Delta z$ in which we define a polarized electric field. $\mathbf{E_{source}} = \mathrm{E_x}\left(\mathrm{x,y}\right)\overrightarrow{i}$. This source impinges on the diaphragm so that a Gaussian beam enters the waveguide itself at $z = 11\Delta z$. The total waveguide length is $15\Delta z$ = 0.665 μm and the number of time steps is 25000, which amounts to a total simulated time of 0.3 10^{-12} s.

Rate equations

In this section, we detail the ADE part of the method which describes the time population dynamics of Si-ng and Nd^3+ levels with the following rate equations.

Silicon nanoclusters

We consider both radiative r and non radiative nr transitions. The optical pumping power (in m^{-3}) writes $\frac{1}{\hbar\omega_p}\mathbf{E}(t)\frac{d\mathbf{P}_p(t)}{dt}$. The energy transfer between Si-ng and

RE ions is described by a transfer coefficient K and equal to $KN^*_{Si}(t)\,N_0(t)$ at time t. This leads to the following rate equations:

$$\frac{dN^*_{Si}(t)}{dt} = +\frac{1}{\hbar\omega_p}\mathbf{E}(t)\frac{d\mathbf{P}_p(t)}{dt} - \frac{N^*_{Si}(t)}{\tau^*|^r_{nr}} - KN^*_{Si}(t)N_0(t), \quad (4)$$

$$\frac{dN_{Si}(t)}{dt} = -\frac{1}{\hbar\omega_p}\mathbf{E}(t)\frac{d\mathbf{P}_p(t)}{dt} + \frac{N^*_{Si}(t)}{\tau^*|^r_{nr}} + KN^*_{Si}(t)N_0(t). \quad (5)$$

Rare earth ions Nd $^{3+}$

A five level scheme is adopted for the Nd^{3+} ion in Figure 2 [9,10].

We consider three radiative transitions ($4F_{3/2} \rightarrow 4I_{9/2}$, λ_{20} = 945 nm; $4F_{3/2} \rightarrow 4I_{11/2}$, λ_{21} = 1064 nm; and $4F_{3/2} \rightarrow 4I_{13/2}$, λ_{24} = 1340 nm) and three non radiative transitions ($4F_{5/2}$ - > $4F_{3/2}$ ($N_3 \mapsto N_2$) $4I_{11/2}$ - > $4I_{9/2}$ ($N_1 \mapsto N_0$) and $4I_{13/2}$ - > $4I_{11/2}$ ($N_4 \mapsto N_1$)).

The terms $+\frac{1}{\hbar\omega_{21}}\mathbf{E}(t)\frac{d\mathbf{P}_{21}(t)}{dt}$, $+\frac{1}{\hbar\omega_{20}}\mathbf{E}(t)\frac{d\mathbf{P}_{20}(t)}{dt}$ and $+\frac{1}{\hbar\omega_{24}}\mathbf{E}(t)\frac{d\mathbf{P}_{24}(t)}{dt}$ correspond to the stimulated transitions 2 → 1, 2 → 0 and 2 → 4. The terms $-\frac{N_2(t)}{\tau_{21}|^r_{nr}}$, $-\frac{N_2(t)}{\tau_{20}|^r_{nr}}$ and $-\frac{N_2(t)}{\tau_{24}|^r_{nr}}$ correspond to the spontaneous transitions 2 → 1, 2 → 0 and 2 → 4.

The associated rate equations read:

$$\frac{dN_3(t)}{dt} = -\frac{N_3(t)}{\tau_{32}|_{nr}} + KN^*_{Si}(t)N_0(t), \quad (6)$$

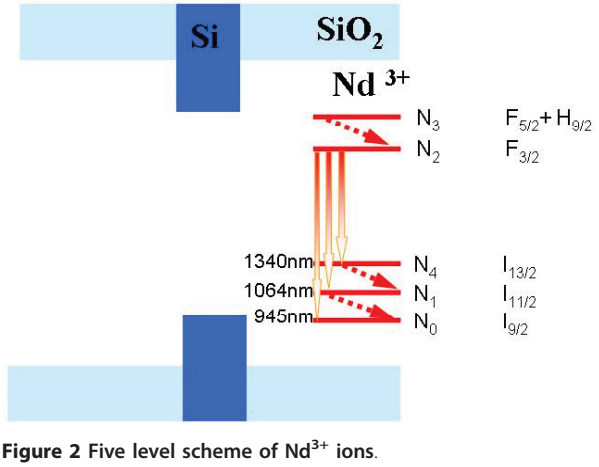

Figure 2 Five level scheme of Nd^{3+} ions.

$$\frac{dN_2(t)}{dt} = \frac{1}{\hbar\omega_{24}}\mathbf{E}(t)\frac{d\mathbf{P}_{24}(t)}{dt} + \frac{1}{\hbar\omega_{21}}\mathbf{E}(t)\frac{d\mathbf{P}_{21}(t)}{dt} + \frac{1}{\hbar\omega_{20}}\mathbf{E}(t)\frac{d\mathbf{P}_{20}(t)}{dt} + \frac{N_3(t)}{\tau_{32}|_{nr}} - \frac{N_2(t)}{\tau_{21}|^r_{nr}} - \frac{N_2(t)}{\tau_{20}|^r_{nr}} - \frac{N_2(t)}{\tau_{24}|^r_{nr}}, \quad (7)$$

$$\frac{dN_4(t)}{dt} = -\frac{1}{\hbar\omega_{24}}\mathbf{E}(t)\frac{d\mathbf{P}_{24}(t)}{dt} + \frac{N_2(t)}{\tau_{24}|^r_{nr}} - \frac{N_4(t)}{\tau_{41}|_{nr}}, \quad (8)$$

$$\frac{dN_1(t)}{dt} = -\frac{1}{\hbar\omega_{21}}\mathbf{E}(t)\frac{d\mathbf{P}_{21}(t)}{dt} + \frac{N_2(t)}{\tau_{21}|^r_{nr}} - \frac{N_1(t)}{\tau_{10}|_{nr}} + \frac{N_4(t)}{\tau_{41}|_{nr}}, \quad (9)$$

$$\frac{dN_0(t)}{dt} = -\frac{1}{\hbar\omega_{20}}\mathbf{E}(t)\frac{d\mathbf{P}_{20}(t)}{dt} + \frac{N_2(t)}{\tau_{20}|^r_{nr}} + \frac{N_1(t)}{\tau_{10}|_{nr}} - KN^*_{Si}(t)N_0(t). \quad (10)$$

Application to rib-loaded waveguide

In table 1, we collect the simulation parameters taken into account for the transitions. The lifetimes correspond to the experimental ones divided by the scaling factor 10^6.

The transfer coefficient K estimated to ~ 10^{-20} m^3 s^{-1} [11] has also been scaled with the same factor 10^6: K = 10^{-14} $m^3.s^{-1}$. The amplitudes of the input pumping and signal electric fields have been taken equal to E_{pump} = 10^7 $V.m^{-1}$ and E_{signal} = 100 $V.m^{-1}$.

After the time Fourier transform of both **E** and **H** fields, we deduce the z component of the pump (R_z^{pump}) and signal (R_z^{signal}) Poynting vectors (in $W.m.^{-2}$)

Three Si-ng concentrations have been investigated (N_{si} = 10^{25}, 10^{24} and 10^{23} m^{-3}). In the initial states, only the ground level is populated. The corresponding (xz) maps (R_z^{pump}) are plotted in Figures 3, 4 and 5.

In these figures, the different calculation box zones may be recognized: *i*) the Perfectly Matched Layer (PML) which lies in the area from the lefthand side between z = 0 nm and z = 180 nm, and from the

Table 1 Simulation parameters of the Si-ng and Nd^{3+} transitions

Transition	lifetime(s)	type	ω_{ij} (s^{-1})	$\Delta\omega_{ij}$ (s^{-1})
Si →Si *	4 10^{-11}	R	3.86 10^{15}	4.4 10^{14}
3 → 2	2.3 10^{-16}	NR		
2 → 0	3 10^{-10}	R	2.07 10^{15}	1.38 10^{14}
2 → 1	3 10^{-10}	R	1.7 10^{15}	1.39 10^{14}
2 → 4	3 10^{-10}	R	1.3 10^{15}	1.33 10^{14}
4 → 1	9.7 10^{-16}	NR		
1 → 0	5.1 10^{-16}	NR		

R and NR stand for radiative and non-radiative transitions respectively.

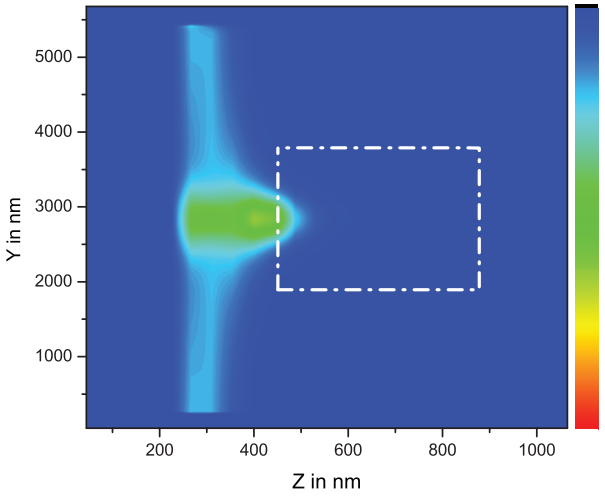

Figure 3 (*yz*) maps of R_z^{pump} in W.m^{-2} for [Si-ng] = 10^{25} m^{-3}, the dashed-dot rectangle represents the waveguide rib.

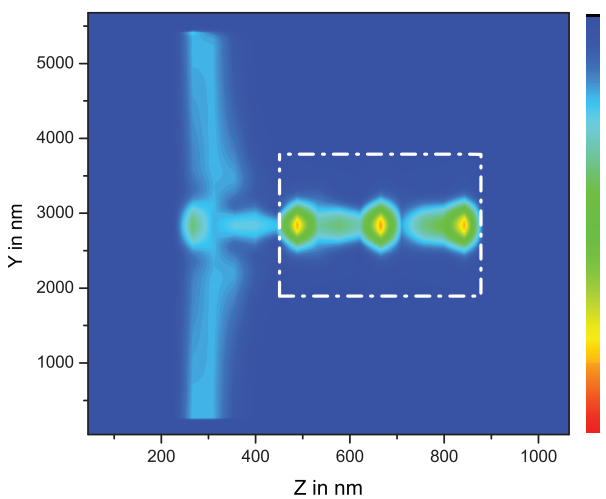

Figure 5 (*yz*) maps of R_z^{pump} in W.m^{-2} for [Si-ng] = 10^{23} m^{-3}, the dashed-dot rectangle represents the waveguide rib.

righthand side between z = 890 nm and z = 1000 nm, *ii*) the plane containing the electromagnetic field source at z ~ 300 nm, *iii*) the FDTD zone which is located at about 180 nm from border of plot, the Gaussian beam impinging in the waveguide at z ~ 500 nm and the intensity propagating in waveguide from z ~ 500 nm to z ~ 900 nm.

On the basis of the parameters taken from experiments, these plots evidence the fact that for Si-ng concentrations above 10^{24} m^{-3}, the pumping wave does not reach the end of the waveguide. This concentration threshold corresponds to high experimental values [12], and is above the lower values leading to minimal optical losses [1].

In order to reduce the computing time, in addition to the scaling method, we start the calculations with Si-ng levels already populated at the maximum inversion rate, $N_{Si} = N_{Si}^* = 5\ 10^{22}$ m^{-3}. Hence, for a given total Si-ng concentration of 10^{23} m^{-3}, this result (Figure 6) can be compared to the preceding one where $N_{Si} = 10^{23}$ m^{-3} and $N_{Si}^* = 0$ (Figure 5). The propagation of the pump power within the waveguide seems to be similarly attenuated in both cases. The main difference occurs in the N_3 level concentration which is directly populated from the excited N_{Si}^* level. In case of maximum inversion rate, the stationary regime is reached and the concentration becomes equal to $N_3 = \tau_{32}.K.N_{Si}^*.N_0 \approx 1.1\ 10^{18}$ m^{-3}. In case of $N_{Si} = 10^{23}$ m^{-3} and $N_{Si}^* = 0$ starting

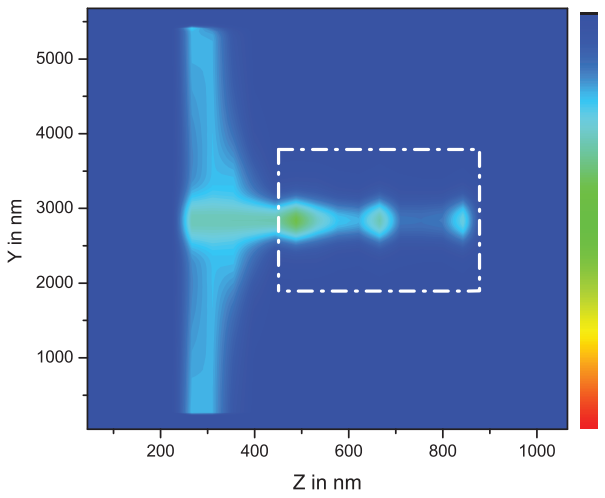

Figure 4 (*yz*) maps of R_z^{pump} in W.m^{-2} for [Si-ng] = 10^{24} m^{-3}, the dashed-dot rectangle represents the waveguide rib.

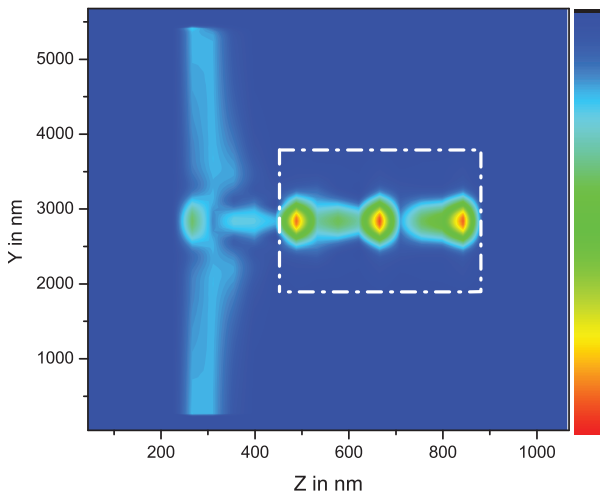

Figure 6 (*yz*) map of R_z^{pump} in W.m^{-2} N_{Si} 5 10^{22} m^{-3}/N_{Si}^* = 5 10^{22} m^{-3}.

concentration, the N_3 concentration does not reach a stationary regime and stays below several 10^{17} m^{-3}.

Conclusion

We have investigated by means of ADE-FDTD method the electromagnetic field propagation in rib-loaded waveguides constituted of an active layer of Nd^{3+} doped silicon rich silica stacked between pure silica bottom cladding and rib. This numerical method treats Nd^{3+} and Si-ng levels rate equations (ADE) coupled to the Maxwell equations (FDTD). The extremely different specific times involved in the ADE (levels lifetimes ≈ 10 μs) and in FDTD (electromagnetic wave periods ≈ 10^{-15} s) have required the use of the scaling time method which allows reasonable computing time: the number of time iterations has been reduced by six orders of magnitude. In addition to this method, we have proposed to start the calculations with steady state Si-ng ground and excited populations. The numerical computation has been performed for several Si-ng concentrations. Therefore we can infer that the pumping wave propagation (λ_{pump} = 488 nm) is possible for [Si-ng] ≤ 10^{24} m^{-3} in agreement with experimental loss measurements. The upper Nd^{3+} level reaches its stationary value predicted with the analytical solution of the steady state rate equations.

Acknowledgements
The authors are grateful to the French Agence Nationale de la Recherche, which supported this work through the Nanoscience and Nanotechnology program (DAPHNES project ANR-08-NANO-005).

Authors' contributions
CD and JC conceived the calculation code, AF carried out most of the calculations, OD performed the optical measurements on our samples and FG conceived the whole project. All authors read and approved the final manuscript.

Competing interests
The authors declare that they have no competing interests.

Received: 27 September 2010 Accepted: 4 April 2011
Published: 4 April 2011

References

1. Navarro-Urrios D, Melchiorri M, Daldosso N, Pavesi L, García C, Pellegrino P, Garrido B, Pucker G, Gourbilleau F, Rizk R: **Optical losses and gain in silicon-rich Silica waveguides containing Er ions.** *Journal of Luminescence* 2006, **121**:249-255.
2. Shi S, Prather DW: **Lasing dynamics of a silicon photonic crystal microcavity.** *Opt Express* 2007, **15(16)**:10294-10302.
3. Redding B, Shi S, Creazzo T, Prather DW: **Electromagnetic modeling of active silicon nanocrystal waveguides.** *Opt Express* 2008, **16**:8792-8799.
4. Berenger JP: **A perfectly matched layer for the absorption of electromagnetic waves.** *J of Computational Physics* 1994, **114(2)**:185-200.
5. Biallo D, De Sario M, Petruzzelli V, Prudenzano F: **Time domain analysis of optical amplification in Er3+ doped SiO2-TiO2 planar waveguide.** *Opt Express* 2005, **13(12)**:4683-4692.
6. Taflove A, Hagness SC, *et al*: **Computational electrodynamics: the finite-difference time-domain method.** *Artech House Norwood, MA* 1995.
7. Zhukovsky SV, Chigrin DN: **Numerical modelling of lasing in microstructures.** *Phys Status Solidi (b)* 2007, **244(10)**:3515-3527.
8. Yee K: **Numerical solution of inital boundary value problems involving Maxwell's equations in isotropic media IEEE Transactions on antennas and propagation.** 1966, **14(3)**:302-307.
9. Serqueira EO, Dantas NO, Monte AFG, Bell MJV: **Judd Ofelt calculation of quantum efficiencies and branching ratios of Nd3+ doped glasses.** *J of Non-Crystalline Solids* 2006, **352(32-35)**:3628-3632.
10. Pecoraro E, Sampaio JA, Nunes LAO, Gama S, Baesso ML: **Spectroscopic properties of water free Nd2O3-doped low silica calcium aluminosilicate glasses.** *J of Non-Crystalline Solids* 2000, **277(2-3)**:73-81.
11. Pacifici Domenico, Franzò Giorgia, Priolo Francesco, Iacona Fabio, Dal Negro Luca: **Modeling and perspectives of the Si nanocrystals-Er interaction for optical amplification.** *Phys Rev B* 2003, **67(24)**:245301.
12. Gourbilleau F, Levalois M, Dufour C, Vicens J, Rizk R: **Optimized conditions for an enhanced coupling rate between Er ions and Si nanoclusters for an improved 1.54-μm emission.** *J Appl Phys* 2004, **95**:3717.

doi:10.1186/1556-276X-6-278
Cite this article as: Dufour *et al.*: Electromagnetic modeling of waveguide amplifier based on Nd^{3+} Si-rich SiO_2 layers by means of the ADE-FDTD method. *Nanoscale Research Letters* 2011 **6**:278.